1.6- and 3.3-W Power-Amplifier Modules at 24 GHz Using Waveguide-Based Power-Combining Structures

Jinho Jeong, *Student Member, IEEE*, Youngwoo Kwon, *Member, IEEE*, Sunyoung Lee, Changyul Cheon, *Member, IEEE*, and Emilio A. Sovero, *Member, IEEE*

***Abstract*—Both 1.6- and 3.3-W power-amplifier (PA) modules were developed at 24 GHz using a waveguide-based power combiner. The combiner is based on a double antipodal finline-to-microstrip transition structure, which also serves as a two-way power combiner. The proposed 1 × 2 combining structure was analyzed and optimized by finite-element-method (FEM) simulations and experiments. An optimized 1 × 2 power combiner showed a very low back-to-back insertion loss of 0.6 dB and return losses better than 17 dB over most of Ka-band. The resonant behavior of the combiner was also identified and analyzed using an FEM simulator. The two-way power-combining approach was extended to four-way (2 × 2) power combining by vertical stacking inside the waveguide. No degradation in the combining efficiency was observed during this process, demonstrating the scalability of the proposed approach. The implemented 1 × 2 power module that combines two 1-W monolithic-microwave integrated-circuit (MMIC) PAs showed an output power of 1.6 W and a combining efficiency of 83% around 24 GHz. The 2 × 2 PA module combining the four 1-W MMICs showed an output power of 3.3 W together with an almost identical combining efficiency. This paper demonstrates the potential of the proposed power combiner for high-power amplification at millimeter-wave frequencies.**

***Index Terms*—Millimeter-wave power amplifiers, power combiners, waveguide transitions.**

I. Introduction

A HIGH power-amplifier (PA) module is one of the most important components in wireless transmitters at microwave and millimeter-wave frequencies. Especially at millimeter-wave frequencies, power available from each monolithic microwave integrated circuit (MMIC) is limited, and subsequent power combining is required to achieve multi-watt-level powers. High-efficiency power combiners with broad bandwidth and good thermal property are essential for this purpose. The waveguide-based power combiner is preferred to coaxial- or planar-type structures as waveguide is a standard medium at millimeter-wave frequencies. Waveguide-based power combiners also offer good heat-sinking property and potential for spatial power combining for massive power combination.

Spatial or quasi-optical power combining is a promising approach that integrates a large number of devices to get watt-level powers at millimeter-wave frequencies. When applied to massive power combination, this method has the potential of achieving higher combining efficiencies than any other conventional planar power-combining schemes. However, a free-space power-combining technique such as grid amplifiers [1] may suffer from diffraction losses, focusing errors, poor heat sinking, and the problems of input/output isolation. Closed-waveguide combiners, where power combining occurs inside the waveguide [2], [3], are more attractive for practical use than free-space combiners, since the former can eliminate or alleviate the problems of the latter. A 25-W Ka-band amplifier and a 36-W V-band source, for example, were developed using quasi-optical power combining in closed waveguides [4], [5]. They showed very high output power at millimeter waves with good thermal sinking property through the use of liquid-cooled thick ground metals.

Recently, waveguide-based spatially combined power amplifiers (PAs) were developed using tapered slot antenna arrays at X-band [6], [7]. They demonstrated a 120-W PA module at X-band by combining 6 × 4 MMIC PAs in a waveguide with a high peak combining efficiency of 88% [8]. For combining the output powers of a large number of MMIC amplifiers, this kind of waveguide-based spatial power combiner is much preferred to planar combining structures such as corporate combiners since the latter suffers from increased losses as the number of PAs increases. The structure presented in [8], however, is rather limited in operating frequencies since it relies on slotline-to-microstrip transitions using bond wires without sophisticated balun structures. The structure, thus, cannot be easily applied to millimeter-wave power applications because of poor reproducibility of wire bonding; the length and shape of the bond wires, which are crucial parameters of the transition, are hard to control with acceptable accuracy at millimeter-wave frequencies. Moreover, accurate modeling of bond wires is nontrivial at this frequency.

In this paper, we propose a waveguide-based power-combining structure at Ka-band using double antipodal finline-to-microstrip transitions. The balun is integrated into the structure and no bond wires are needed in mode transition. The structure, therefore, allows improved efficiency and excellent repeatability at millimeter waves. A proposed 1 × 2 combining

Manuscript received March 6, 2000; revised August 25, 2000. This work was supported by the Korean Ministry of Science and Technology under the Creative Research Initiative Program.

J. Jeong and Y. Kwon are with the School of Electrical Engineering, Seoul National University, Seoul 151-742, Korea.

S. Lee and C. Cheon are with the Department of Electronics, University of Seoul, Seoul 130-743, Korea.

E. A. Sovero is with the Rockwell International Science Center, Thousand Oaks, CA 91360 USA.

Publisher Item Identifier S 0018-9480(00)10749-5.

structure was analyzed and optimized by FEM simulations and experiments. The two-way power combiner was also extended to a four-way (2 × 2) combiner by vertical stacking. The 1 × 2 and 2 × 2 power modules combining 1-W MMIC PAs have been implemented to demonstrate multiple watt power modules at millimeter-wave frequencies. The 1 × 2 power module showed an output power of 32.2 dBm and the 2 × 2 power module showed 35.2 dBm at 24 GHz with high combining efficiencies of 83%. The details of the proposed 1 × 2 power combiner are presented in Section II, followed by the extension to a 2 × 2 combiner in Section III. Construction and measured performance of the 1.6- and 3.3-W power modules are presented in Section IV.

II. Proposed Power-Combining Structure

A. Operation Principle of the Proposed Power Combiner

The proposed power combiner is based on a waveguide-to-microstrip transition using antipodal finlines [9]. Antipodal finlines translate the TE_{10} mode of the rectangular waveguide to the quasi-TEM mode of the microstrip line by rotating the electric field. In terms of impedance, they transform the high impedance of the waveguide to the low impedance of the microstrip line. In this paper, a double antipodal finline-to-microstrip transition structure, where two transitions sit side by side, was adopted to implement a power-combining function as well as mode transition.

The proposed power-combining structure is shown in Fig. 1. Two waveguide-to-antipodal finline-to-microstrip transitions are integrated on a single substrate, which are then inserted into the central E-plane of the waveguide. The stryucture thus operates as a two-way power combiner. Fig. 1(c) illustrates the principle of mode transition and antiphase equal power division (3 dB). In the region between points a and b in Fig. 1(a), the tapered antipodal finline gradually rotates the vertical electric field of TE_{10} mode to the lateral direction. Also happening in this region is the impedance transformation from the high impedance of the waveguide to the low one of the microstrip line. By the time the wave reaches point c, the E-field has been rotated by 90°, and has almost matched the E-field profile and impedance of the microstrip lines. However, the field profile at point c is still asymmetric with broader field extension to one side of the microstrip line. This can be solved by employing a balun structure, which is implemented by gradually flaring the ground plane from point c to point d. Finally, by point d, the field has become the quasi-TEM mode of microstrip lines, and antiphase equal power division has been achieved.

Also shown in Fig. 1(b) is the detailed layout of the combiner arranged in the back-to-back configuration for testing. The dielectric impedance transformer (DIT) is integrated in the substrate to transform the impedance of the air-filled waveguide to that of partially dielectric-filled waveguide where the finline transition begins. The exponential taper was adopted for this purpose, and the geometry of the impedance transformer was determined using the impedance equations of partially dielectric-filled waveguide [10]. The resulting exponential impedance taper turned out to be almost triangular in shape. DIT improved the return loss by 2∼3 dB in the measurement.

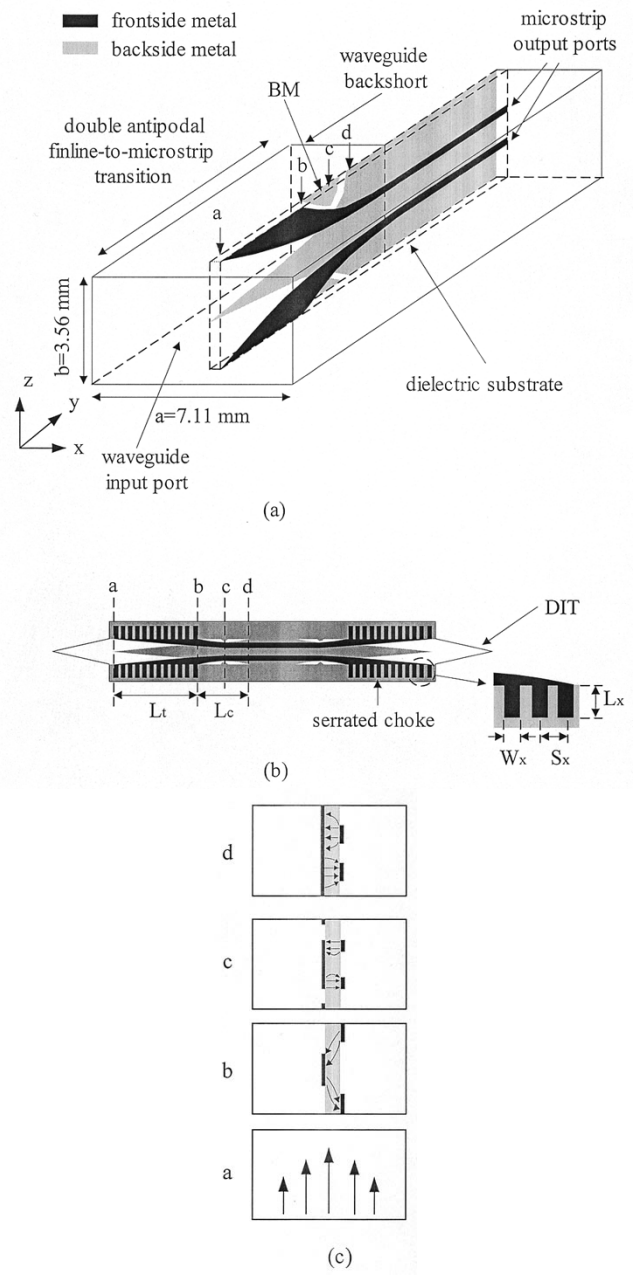

Fig. 1. Proposed power combiner. (a) 3-D view of the structure. (b) Detailed substrate layout (back-to-back). (c) E-field profiles at various points along the length of the transition.

Fig. 1(b) also shows serrated chokes that were employed to bring the frontside finline into an electrical contact with the waveguide wall. Chokes consist of the quarter-wave length microstrip open-stub arrays, which enforce short boundary conditions at the waveguide wall. The backside finline, on the other hand, was hard contacted by conductive epoxy. The use of serrated chokes allowed us to avoid hard contacting both sides of the substrate to the waveguide wall at the same time. This helped to solve the repeatability problems caused by poor contact when attempting to press fit both sides to make contacts. To minimize reflections and losses due to the chokes, the length (L_x), width

(W_x), and pitch (S_x) of the chokes were optimized by repetitive experiments.

Compared to the single antipodal finline-to-microstrip transition, the double antipodal finline structure is expected to show broader bandwidth due to a reduced impedance transformation ratio. Conventional waveguide-to-finline transition often suffers from restricted bandwidth due to a high-impedance transformation ratio between the waveguide and the microstrip line ($>8:1$). Since the impedance seen by each finline transition at the waveguide end is halved in the double finline structure, the bandwidth problem can, in principle, be alleviated.

B. Analysis and Design of the Proposed Power Combiner

The initial structure design was performed using a custom three-dimensional (3-D) vector finite-element method (FEM) structure simulator developed by the authors [11]. In the analysis, we assume that only TE_{10} mode exists at the boundary of waveguide port. At the boundary where microstrip line terminates, we use perfect matched layers to implement the matched port conditions. The complex permittivities and permeabilities of the layers are chosen carefully not to trigger any reflections at the boundary. All conducting materials including the waveguide walls, microstrip line, and ground plane are assumed to be perfect electric conductors.

After the initial design, the structure was optimized experimentally by adjusting the key parameters. For this purpose, the following key parameters were first identified:

1) length of the transition L_t;
2) length of the semicircular cutout L_c;
3) width (W_x);
4) pitch (S_x);
5) length (L_x) of the serrated chokes.

These parameters are specified in Fig. 1(b). As mentioned earlier, field rotation and impedance transformation take place in the region between points a and b. L_t denotes the length of this region, i.e., the transition length. The longer the transition region is, the less the reflection is. However, low reflection comes at the cost of increased insertion loss due to ohmic losses. L_t, therefore, needs to be compromised between the return and insertion loss. Another set of the parameters of importance belongs to the serrated chokes. The length (L_x), width (W_x), and pitch (S_x) determine the effectiveness of the electrical ground and have to be optimized carefully.

The most sensitive parameter in the structure is L_c, the length of the semicircular cutout. This parameter determines the length of the balun [region between points c and d in Fig. 1(b)] and should, therefore, be determined appropriately to ensure smooth transition. Moreover, L_c also controls the frequency of the in-band resonance that is often observed in the antipodal finline transitions. Fig. 2(a) shows the insertion and return loss of the back-to-back connected double antipodal finline structure for two different choices of L_c ($L_{c1} = 8.3$ mm, and $L_{c2} = 8.9$ mm). For both cases, resonant behavior is observed near the center of the Ka-band. The resonance is attributed to the semicircular cutout region that acts like a quasi—2-D cavity. Fig. 3 shows the electric-field profile inside

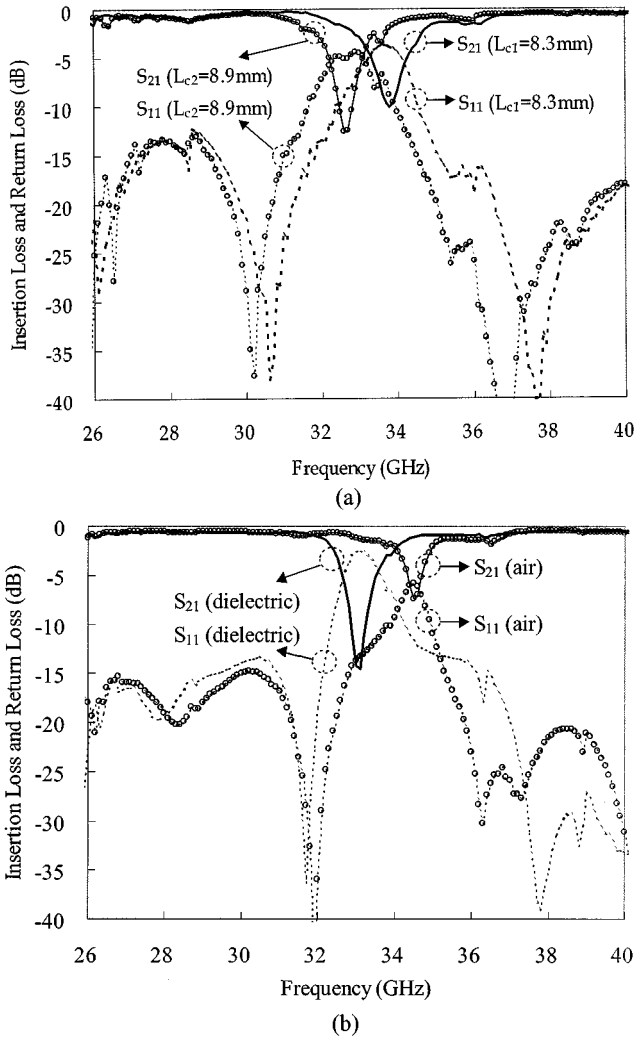

Fig. 2. Measured characteristics of the back-to-back connected 1 × 2 combiner illustrating the resonance frequency shift according to: (a) the length of the semicircular region L_c and (b) the effective dielectric constant of the resonant region.

the substrate at the central E-plane of waveguide for two cases: one at the resonance and the other off the resonance. The field profile at the resonant frequency (31.7 GHz) is shown in Fig. 3(a) (magnitude of the total E-field intensity) and Fig. 3(b) (z-axis component of the E-field). It can be observed from Fig. 3(a) and (b) that the E-field is heavily concentrated in the semicircular cutout region, and that the most dominant E-field component in this region is the z-axis component. The leaky wave from the transition region is believed to generate z-axis component of the electric field and trigger resonance in the semicircular region in the same way as in a two-dimensional (2-D) slot cavity. In this simulation, L_c was set to 9.5 mm, corresponding approximately to one guided wavelength at 31.7 GHz. Two local maximum points of electric-field intensity were found along the semicircular cutout region, which is in accordance with the guided wavelength considerations. Fig. 3(c) shows the nonresonant case (36.0 GHz) with a low back-to-back insertion loss of 0.54 dB. E-field intensity in the

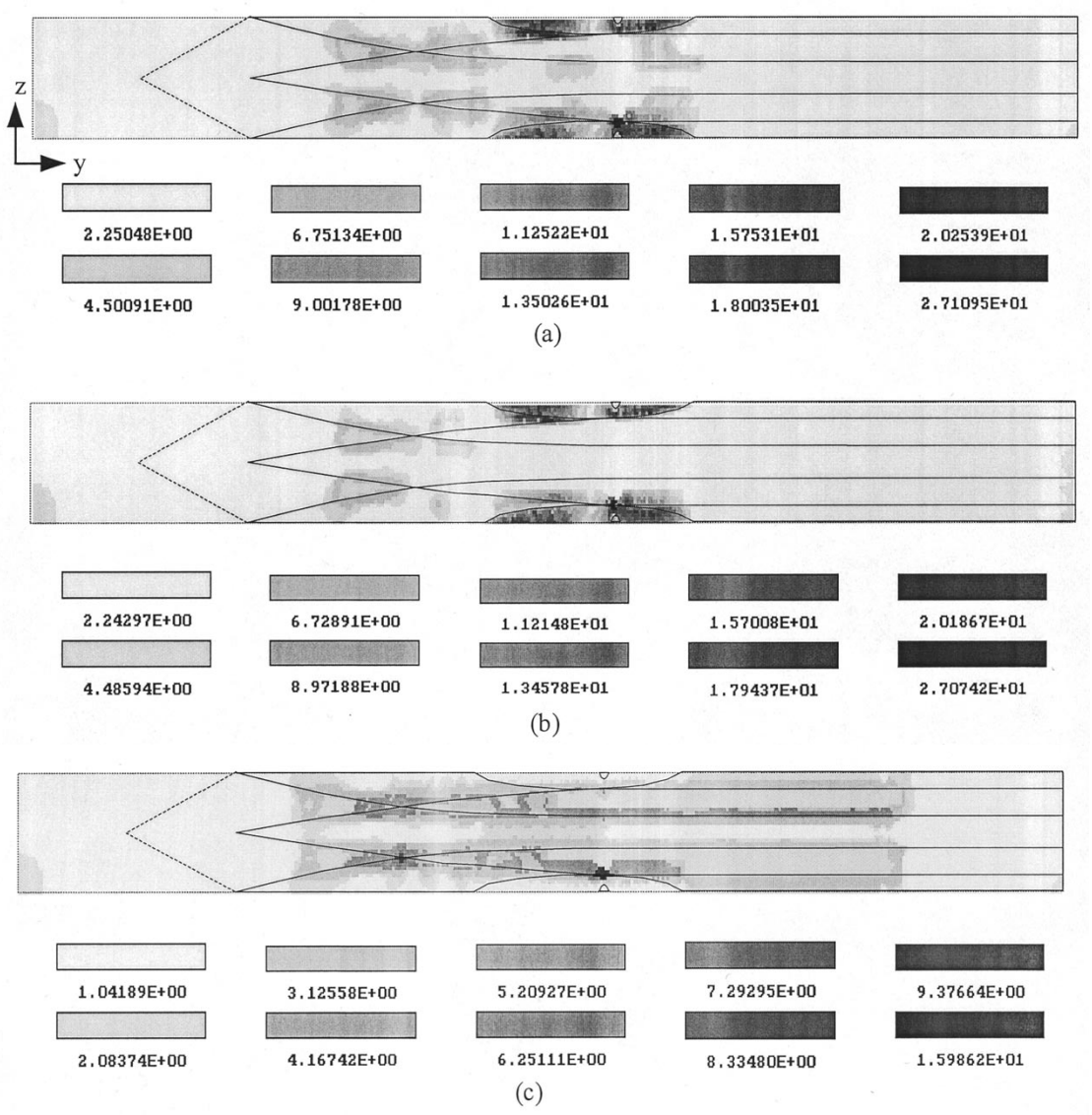

Fig. 3. Electric-field intensity profile inside the dielectric substrate ($x = 3.56$ mm on yz-plane). (a) Magnitude of total electric-field intensity at the resonant frequency. (b) Magnitude of z-axis component of the E-field at the resonance frequency. (c) Magnitude of total electric-field intensity at off-resonance frequency. The units of the E-field intensity is volts per meter.

resonant region is weak and the field is well confined within the microstrip lines.

Based on the field analysis, it can be easily inferred that the resonant frequency can be controlled by simply adjusting the length of the semicircular cavity (L_c), which was indeed the case, as shown in Fig. 2(a). The longer L_c becomes, the lower down the resonance frequency goes. It is worthwhile to note that the resonant frequency can also be changed by adding the backside metal [referred to as "BM" in Fig. 1(a)], which modifies the shape of semicircular cutout and changes the resonant frequency; adding the backside metal decreased the resonant frequency. Similar trends were reported by the authors for the conventional waveguide-to-microstrip transition [12]. In addition, Fig. 2(b) shows that the resonant frequency can also be controlled by modifying the effective dielectric constant of semicircular region. For this purpose, the substrate material in the semicircular region was selectively removed by cutting. In Fig. 2(b), "air" refers to the case where the dielectric in the semicircular region was removed. Reduced effective dielectric constant in the "air" case increased the resonant frequency from 32.8 to 34.5 GHz.

After repetitive experiments with slight adjustment of the key parameters, an optimum Ka-band power-combiner design was obtained, and the final structure was fabricated on a 10-mil-thick Duroid substrate ($\text{dielectric constant} = 2.2$). Fig. 4 shows the measured characteristics of the optimum 1×2 back-to-back connected power combiner. Also shown in Fig. 4 is the calculated insertion loss obtained from the custom FEM simulator. The FEM simulator predicts well the resonance frequency and insertion-loss characteristics. The measured insertion loss including the losses of the microstrip lines was less than 0.6 dB and the return loss was better than 17 dB across the entire Ka-band, except for the frequencies between 32–35 GHz, where the resonance occurs. Since the main purpose of this paper is to demonstrate the power-combining capability of the proposed structure, no attempt was made to push the resonance out of the band.

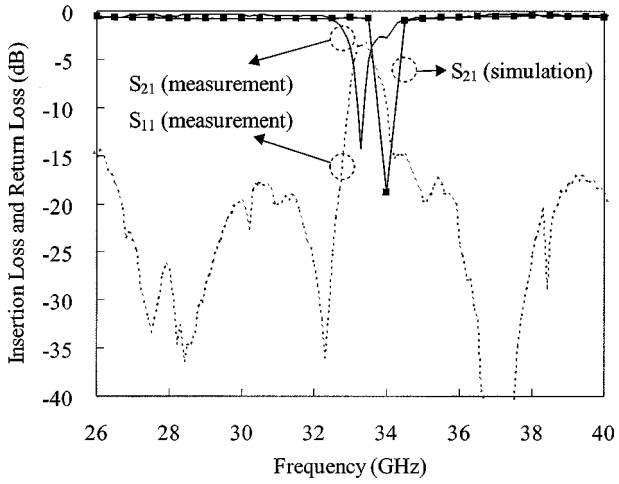

Fig. 4. Measured and simulated performance of the back-to-back 1 × 2 power combiner optimized for broad-band operation at Ka-band.

III. Extension to 2 × 2 Power-Combining Structure

The proposed 1 × 2 combiner can, in principle, be extended to 1 × $2n$ combiner to accommodate $2n$ MMICs by employing n double antipodal finline transitions on the same substrate. However, the number of MMICs that can be integrated on a single substrate is practically limited by the physical size of MMICs and waveguides, as well as thermal issues. To accommodate many MMICs, the microstrip lines need to be meandered. However, long lines result in increased losses as in the case of conventional corporate combining and, therefore, defeats the purpose of spatial combining. The size restrictions due to waveguides can be alleviated by using oversized waveguides, which is, however, limited by overmoding effects.

A 2-D waveguide-based spatial power combiner, where several planar power combining trays are vertically stacked in the E-plane of waveguide, has been proposed in [6]–[8]. This structure is very useful for massive power combining since it is capable of combining multiple one-dimensional (1-D) power trays without much degradation in the combining efficiency. In this paper, a similar stacking method was employed to extend the 1 × 2 double antipodal finline power combining approach to a 2 × 2 power-combining array.

Fig. 5 shows the stacking configuration used in this paper. It is a two-tray system, where two identical 1 × 2 power combiners described in the previous section are inserted in the E-plane of WR-28 waveguide with a spacing of 1.9 mm. The combiner consists of three metal blocks, a central piece containing the two 1 × 2 combining trays, and the remaining two pieces to complete the waveguide. The ground planes of each tray were placed face to face to each other so that the interactions between MMIC PAs could be minimized.

Fig. 6 shows the simulated and measured results of the back-to-back connected 2 × 2 power combiner. Unlike the aforementioned 1 × 2 combiner that was designed to demonstrate the broad-band power-combining capability at Ka-band, the 2 × 2 structure was constructed with a special purpose; it was designed to actually combine the output powers of the 1-W Ka-band MMICs developed by the authors [13]. Hence, the

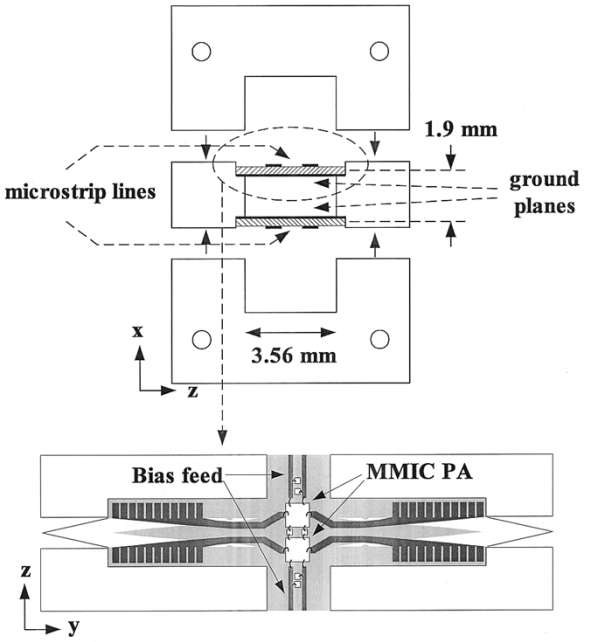

Fig. 5. Schematic diagram of the 2 × 2 power combiner showing the stacking method and construction.

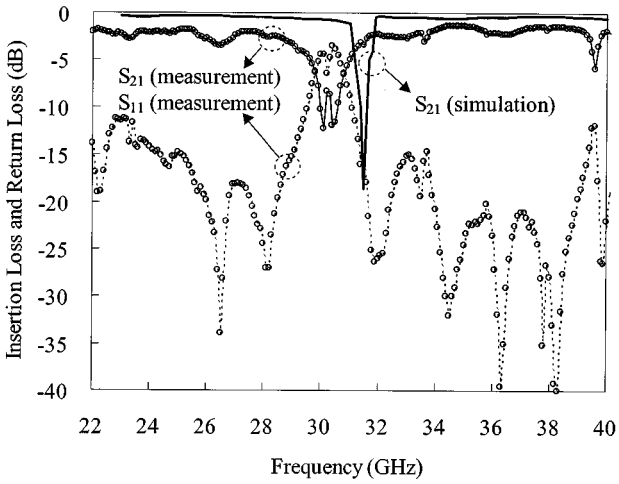

Fig. 6. Simulated and measured results of the back-to-back connected 2 × 2 power combiner used for actual power combining. This 2 × 2 combiner was optimized for 24-GHz operation and had longer microstrip lines to accommodate the MMIC chips.

2 × 2 structure was optimized to show the best performance at 24 GHz, which happened to be the frequency where the MMIC PAs had highest gain. Unfortunately, somewhat poor combiner performance was unavoidable at 24 GHz since it was close to the waveguide cutoff; the recommended frequency range of WR-28 waveguide was from 26.5 to 40 GHz. On top of that, the microstrip pattern in the 2 × 2 combiner had to be meandered to accommodate the large MMIC chips for mounting. In this way, the line lengths were made longer and higher conductor losses were inevitable. Measured insertion loss was 2.0 dB around 24 GHz and 1.8 dB across the Ka-band, except for the resonant frequencies. Simulated loss was 1.5 dB smaller than the measured one since the conductor loss was not taken into account during the simulation.

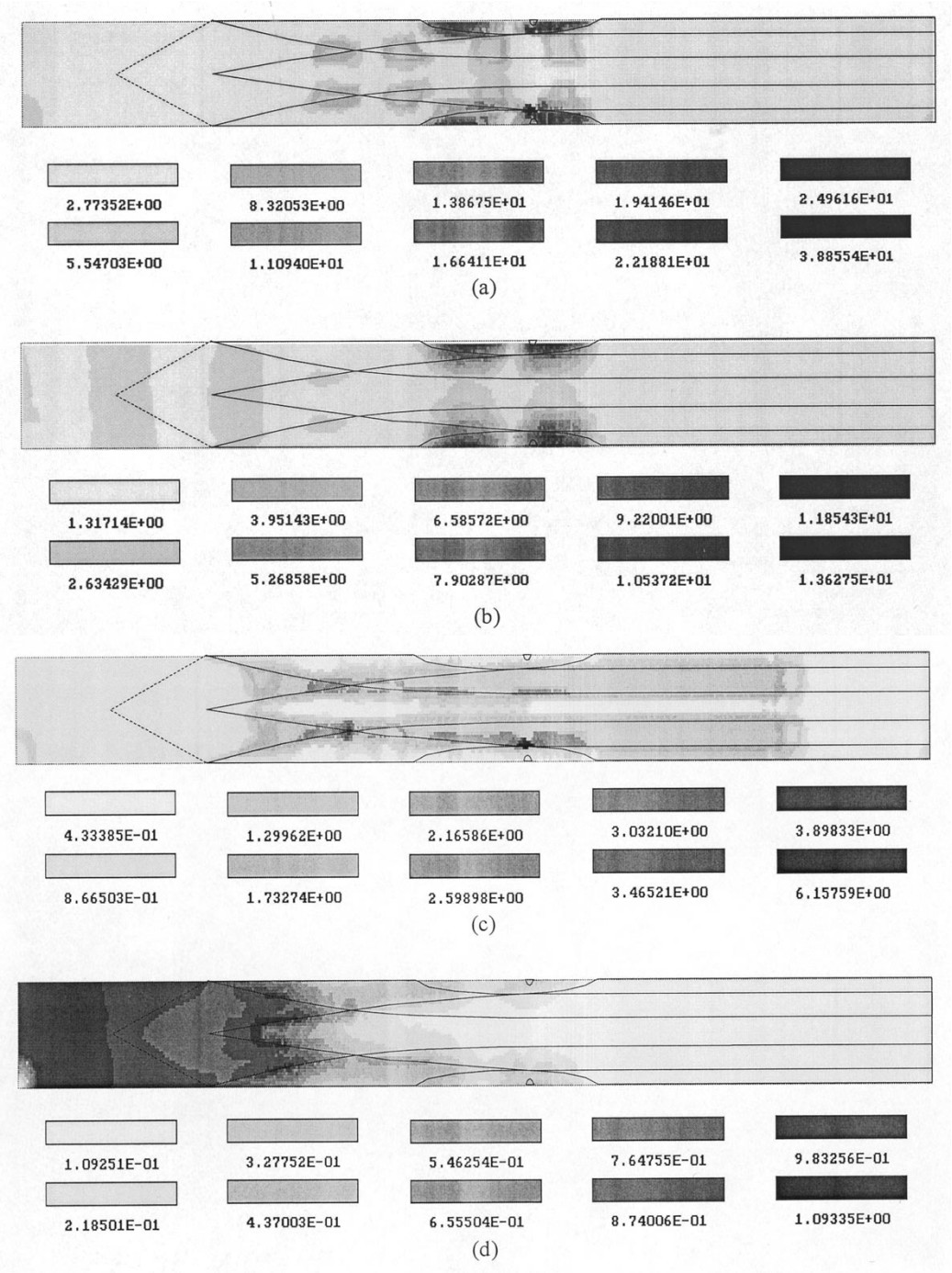

Fig. 7. Electric field profiles of 2 × 2 power combiner. (a) Inside the substrate at the resonance frequency. (b) In between trays at the resonance frequency. (c) Inside the substrate at the off-resonant frequency. (d) In between trays at the off-resonance frequency. The units of the E-field intensity is in volts per meter.

In order to tell the effect of stacking apart, a 1 × 2 combiner with the same metal pattern as the 2 × 2 combiner was also fabricated and measured. Relative performance degradation in the 2 × 2 combiner compared to this 1 × 2 combiner can, in this way, be solely attributed to the effect of vertical stacking. The fabricated 1 × 2 combiner showed a measured insertion loss of 1.6 dB around 24 GHz and 1.2 dB across the band, which were less than 0.4-dB difference at the frequency of interest, illustrating almost negligible deleterious effect due to vertical stacking. To be sure, field simulations were also performed to double check whether any unwanted modes were excited in between the trays. Fig. 7 shows the electric-field profiles inside the substrate of one tray [see Fig. 7(a) and (c)] and in between the trays along the central E-plane of the waveguide [see Fig. 7(b) and (d)]. Fig. 7(a) and (b) corresponds to the field profiles at the resonant frequency (31.5 GHz), while Fig. 7(c) and (d) are near the off-resonant frequency (24.0 GHz). At the off-resonant frequencies, the electric field in between the trays is negligible with a field strength only 1/10 of that inside the substrate. Similar trends are observed at the resonant frequencies; very weak field is observed in between the trays. However, for the areas beneath the semicircular cutout region, strong localized fields

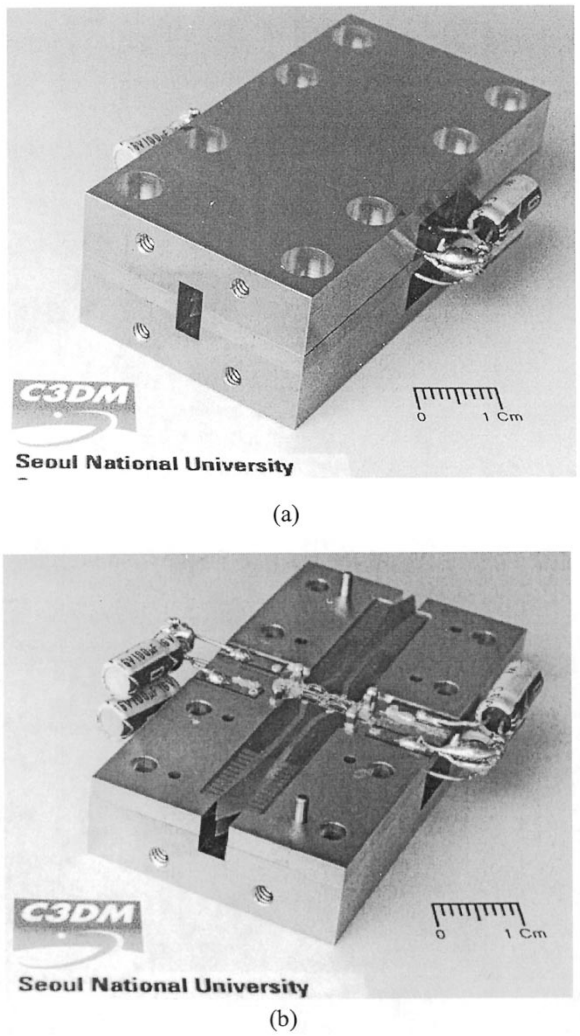

Fig. 8. 2 × 2 power module. (a) Overview (b) Inside the combiner with the top removed.

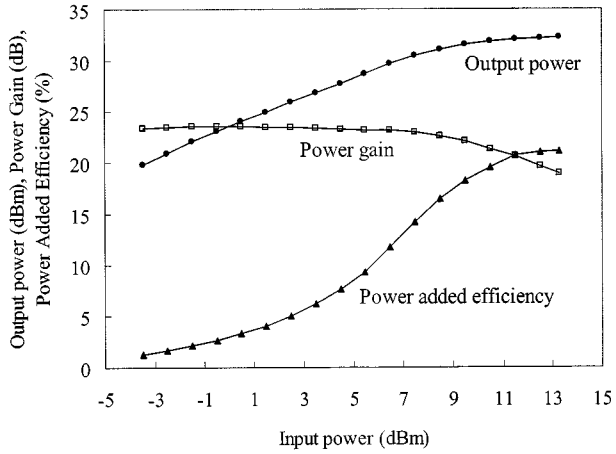

Fig. 9. Measured output power, power gain, and PAE of the 1 × 2 PA module as a function of the input power at 24.2 GHz. Drain bias was 4 V for this measurement.

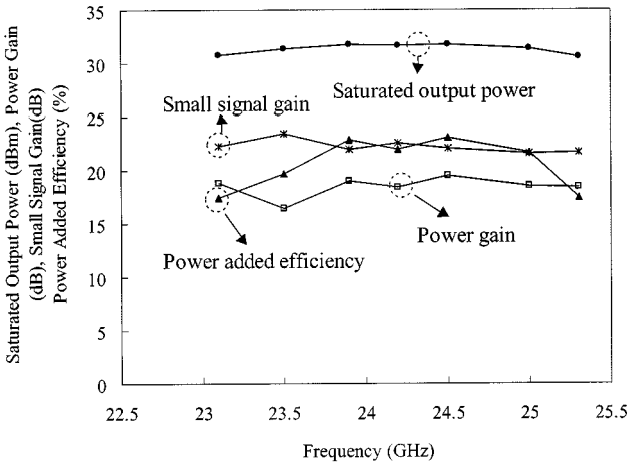

Fig. 10. Measured output power, power gain, small-signal gain, and PAE of the 1 × 2 PA module as a function of the frequency. The drain bias was 3.5 V for this measurement.

are observed at resonant frequencies [see Fig. 7(b)]. Similarity of the field profiles in the resonant region between the trays [see Fig. 7(b)] to that inside the substrate [see Fig. 7(a)] suggests that the localized fields in between the trays be just leakage fields from the quasi-2-D resonator formed inside the tray. Overall, it was shown from both simulation and experiment that vertical stacking could be performed with minor, if any, performance degradation. This demonstrates the excellent scalability of the proposed power combiner design.

IV. 1.6- AND 3.3-W PA MODULE

To demonstrate the combining efficiency of the proposed 1 × 2 and 2 × 2 power-combining structures, 2-W (1 × 2) and 4-W (2 × 2) PA modules were built using 1-W Ka-band MMIC PA chips developed by the authors [13]. MMIC PA chips showed an output power of 1 W at the chip level together with a high power-added efficiency (PAE) of 25%. They were mounted on the test fixture with conductive silver epoxy or indium solder to allow good heat sinking. Thick metal carriers and housing serve as efficient heat sinks. Other approaches such as active cooling can be utilized [4] to further reduce the thermal problems. Gold wires with a diameter of 1.0 mil were used for RF and dc interconnection. Various metal–insulator–metal (MIM) and chip capacitors were mounted along the bias lines to prevent low-frequency oscillations. An overview of the complete 2 × 2 power module is shown in Fig. 8(a), along with the layouts of the tray in Fig. 8(b).

Measured output power and PAE of the 1 × 2 PA module that combines two 1-W MMIC PAs is shown in Fig. 9 as a function of the input power. The frequency was 24.2 GHz. The drain bias was 4.0 V and the gate bias was −0.3 V. The saturated power is 32.2 dBm with an associated gain of 19.0 dB. The peak PAE was 21.1%. The power-combining efficiency was thus estimated to 83%, including the losses of the bond wires and microstrip-to-waveguide transitions. Fig. 10 shows the measured output power, PAE, power gain, and small-signal gain as a function of frequency. The drain bias was reduced to 3.5 V for this frequency sweep. From 23.5 to 25.0 GHz, the average saturation output power is 31.6 dBm with a power gain of 18.9 dB

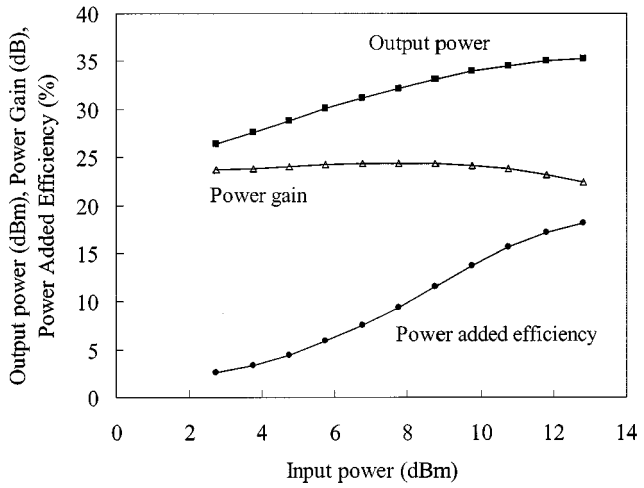

Fig. 11. Measured output power, power gain, and PAE of the 2 × 2 PA module as a function of the input power at 24.1 GHz. The drain bias was 4.5 V for this measurement.

and a PAE of 21.7%. The bandwidth of the power module is entirely limited by that of the MMIC amplifier; the bandwidth of the MMIC chip was about 7%.

A 2 × 2 PA module that combines four 1-W MMIC PAs was constructed by stacking two identical 1 × 2 PA trays as stated in the previous section. Fig. 11 shows the measured output power, power gain, and PAE of the 2 × 2 power module as a function of the input power at 24.1 GHz. The drain bias was 4.5 V and the gate bias was −0.4 V. The measured output power was 35.2 dBm with an associated gain of 22.4 dB, corresponding to a 1.2-dB compression point. The PAE at this power level was 18.1%. The estimated power-combining efficiency was thus about 83%, which again demonstrates virtually no degradation in the combining efficiency by vertical stacking. The power bandwidth of the module as judged from 1-dB variation in the output power was about 1 GHz, which was primarily limited by the bandwidth of the MMICs. This result demonstrates the feasibility of the proposed power combiner as a building block for multi-watt-level PAs at millimeter-wave frequencies.

V. Conclusions

A waveguide-based power-combining structure applicable to millimeter-wave power amplifications has been developed. The combiner employs double antipodal finline transitions to achieve two-way power combining. It, therefore, doubles in function as a broad-band microstrip-to-waveguide transition. The structure was initially analyzed and designed by FEM simulation, and later optimized by repetitive experiments. An optimized Ka-band 1 × 2 power-combining structure showed a very low back-to-back loss of less than 0.6 dB over most of the Ka-band. Despite broad-band characteristics, in-band resonance was found, and has been carefully analyzed using field simulations. The resonance was found to arise from the quasi-2-D cavity formed in the semicircular cutout region in the combiner. The resonance frequency, however, was found to be controllable by changing the dimension of the cavity, and could also be pushed out of the band if needed.

The 1 × 2 power-combining approach based on double antipodal finlines was extended to a 2 × 2 combiner by vertical stacking. Two identical 1 × 2 combiner trays were inserted into the E-plane of the waveguide for this purpose. The 2 × 2 combiner designed for power combination of 24-GHz PA MMICs showed a back-to-back insertion loss of 2.0 dB at 24 GHz, which was almost identical to the loss of the 1 × 2 combiner with the same layout. The scalability of the proposed power-combiner concept was confirmed in this way.

The 1 × 2 and 2 × 2 power combiners were used to combine the output powers of 1-W MMIC PAs to achieve 2- and 4-W power modules at 24 GHz, respectively. The 1 × 2 power module combining two MMICs showed an output power of 1.6 W and a high power-combining efficiency of 83% around 24 GHz. The 2 × 2 PA module implemented by staking two 1 × 2 power modules showed a high output power of 3.3 W and combining efficiency of 83% at 24 GHz. No appreciable degradation in the combining efficiency was found during vertical stacking, which again illustrates that the proposed power-combining approach can be scaled to a higher degree of power combining without further loss.

Extending the operation frequency of the combiner above Ka-band is under way. Since the one-tray combiner is basically composed of finline-to-microstrip transitions, which have been verified up to W-band, it is expected to work without tremendous loss degradation up to 100 GHz. However, the number of the trays in vertical stacking can eventually be limited at high frequencies by the physical size of the waveguide and the thickness of the substrate unless overmoded waveguide is used. Thin low-loss substrates such as 5-mil-thick quartz can be used to alleviate this problem. Overall, the proposed power combiner stands as a strong candidate for medium-to-high power amplification with high efficiency at millimeter-wave frequencies.

References

[1] R. A. York and Z. B. Popović, *Active and Quasi-Optical Arrays for Solid-state Power Combining*. New York: Wiley, 1997.

[2] J. A. Higgins, E. A. Sovero, and W. J. Ho, "44-GHz monolithic plane wave amplifiers," *IEEE Microwave Guided Wave Lett.*, vol. 5, pp. 347–348, Oct. 1995.

[3] Y. Kwon, E. A. Sovero, D. S. Deakin, and J. A. Higgins, "A 44-GHz monolithic waveguide plane-wave amplifier with improved unit cell design," *IEEE Trans. Microwave Theory Tech.*, vol. 46, pp. 1237–1241, Sept. 1998.

[4] S. Ortiz, J. Hubert, L. Mirth, E. Schlech, and A. Mortazawi, "A 25 watt and 50 watt Ka-band quasi-optical amplifier," in *IEEE Int. Microwave Symp. Dig.*, 2000, pp. 797–800.

[5] J. J. Sowers *et al.*, "A 36 W, V-band, solid state source," in *IEEE Int. Microwave Symp. Dig.*, 1999, pp. 235–238.

[6] N.-S. Cheng, A. Alexanian, M. G. Case, D. B. Rensch, and R. A. York, "40-W CW broad-band spatial power combiner using dense finline arrays," *IEEE Trans. Microwave Theory Tech.*, vol. 47, pp. 1070–1076, July 1999.

[7] A. Alexanian and R. A. York, "Broadband spatially combined amplifier array using tapered slot transitions in waveguide," *IEEE Microwave Guided Wave Lett.*, vol. 7, pp. 42–44, Jan. 1997.

[8] N.-S. Cheng, P. Jia, D. B. Rensch, and R. A. York, "A 120-W X-band spatially combined solid-state amplifier," *IEEE Trans. Microwave Theory Tech.*, vol. 47, pp. 2557–2561, Dec. 1999.

[9] J. H. C. Van Heuven, "A new integrated waveguide-microstrip transition," *IEEE Trans. Microwave Theory Tech.*, vol. MTT-24, pp. 144–147, Mar. 1976.

[10] C. J. Verver and W. J. R. Hoefer, "Quarter-wave matching of waveguide-to-finline transitions," *IEEE Trans. Microwave Theory Tech.*, vol. MTT-32, pp. 1645–1648, Dec. 1984.

[11] Y. Jang, J. Jeong, C. Jeong, C. Cheon, and Y. Kwon, "Numerical analysis and design of waveguide-microstrip transition in millimeter-wave band," *Trans. Korean Inst. Elect. Eng.*, vol. 47, no. 11, pp. 2007–2012, Nov. 1998.
[12] J. Jeong, Y. Kwon, Y. Jang, and C. Cheon, "Design and fabrication of rectangular waveguide-to-microstrip transition at Ka-band," *J. Korean Inst. Commun. Sci.*, pp. 1770–1776, 1998.
[13] E. A. Sovero, D. S. Deakin, J. Hong, and Y. Kwon, "Watt level GaAs pHEMT power amplifiers 26 GHz and 40 GHz for wireless applications," in *IEEE Radio Wireless Conf.*, Aug. 1999, pp. 309–312.

Jinho Jeong (S'00) was born in Korea, in 1973. He received the B.S. and M.S. degrees in electrical engineering from the Seoul National University, Seoul, Korea, in 1997 and 1999, respectively, and is currently working toward the Ph.D. degree at the Seoul National University.

His research interests include millimeter-wave power combining, large-signal modeling of microwave transistors and MMIC design.

Youngwoo Kwon (S'90–M'94) was born in Korea, in 1965. He received the B.S. degree in electronics engineering from the Seoul National University, Seoul, Korea, in 1988, and the M.S. and Ph.D. degrees in electrical engineering from The University of Michigan at Ann Arbor, in 1990 and 1994, respectively.

From 1994 to 1996, he was with the Rockwell Science Center, where he was involved in the development of various millimeter-wave monolithic integrated circuits based on high electron-mobility transistors (HEMTs) and heterojunction bipolar transistors (HBTs). In 1996, he joined the faculty of the School of Electrical Engineering, Seoul National University. His current research activities include the design of MMICs for mobile communication and millimeter-wave systems, large-signal modeling of microwave transistors, application of micromachining techniques to millimeter-wave systems, nonlinear noise analysis of MMICs, and millimeter-wave power combining.

Sunyoung Lee was born in Korea, in 1976. She received the B.S. degrees in the electrical engineering from the University of Seoul, Seoul, Korea, in 1999, and is currently working toward the M.S. degree at the University of Seoul.

Her research interests include design of millimeter-wave power combiners using the numerical method.

Changyul Cheon (S'87–M'90) was born in Seoul, Korea, on April 5, 1960. He received the B.S. and M.S. degrees in electrical engineering from Seoul National University, Seoul, Korea, in 1983 and 1985, respectively, and the Ph.D. degree in electrical engineering from The University of Michigan at Ann Arbor, in 1992.

From 1992 to 1995, he was with the Department of Electrical Engineering, Kangwon National University, Chuncheon, Korea, as an Assistant Professor. He is currently an Associate Professor of electrical engineering at the University of Seoul (UoS), Seoul, Korea, where his group is currently involved with the design and analysis of microwave and millimeter-wave passive device using FEM, finite-difference time-domain (FDTD), and method of moments (MoM) techniques. He is also interested in high-power microwave systems for military and commercial applications.

Emilio A. Sovero (M'85), photograph and biography not available at time of publication.